First-passage-probability analysis of active transport in live cells

David A. Kenwright,[1,2] Andrew W. Harrison,[1,2,3] Thomas A. Waigh,[1,3,*] Philip G. Woodman,[2] and Victoria J. Allan[2,3,†]
[1]*Biological Physics, School of Physics and Astronomy, University of Manchester, Manchester M13 9PL, United Kingdom*
[2]*Faculty of Life Sciences, University of Manchester, Manchester M13 9PT, United Kingdom*
[3]*The Photon Science Institute, University of Manchester, Manchester M13 9PL, United Kingdom*
(Received 20 December 2011; published 11 September 2012)

The first-passage-probability can be used as an unbiased method for determining the phases of motion of individual organelles within live cells. Using high speed microscopy, we observe individual lipid droplet tracks and analyze the motor protein driven motion. At short passage lengths ($<10^{-2}\mu$m), a log-normal distribution in the first-passage-probability as a function of time is observed, which switches to a Gaussian distribution at longer passages due to the running motion of the motor proteins. The mean first-passage times ($\langle t_{\mathrm{FPT}}\rangle$) as a function of the passage length (L), averaged over a number of runs for a single lipid droplet, follow a power law distribution $\langle t_{\mathrm{FPT}}\rangle \sim L^{\alpha}$, $\alpha > 2$, at short times due to a passive subdiffusive process. This changes to another power law at long times where $1 < \alpha < 2$, corresponding to sub-ballistic superdiffusive motion, an active process. Subdiffusive passive mean square displacements are observed as a function of time, $\langle r^2\rangle \sim t^{\beta}$, where $0 < \beta < 1$ at short times again crossing over to an active sub-ballistic superdiffusive result $1 < \beta < 2$ at longer times. Consecutive runs of the lipid droplets add additional independent Gaussian peaks to a cumulative first-passage-probability distribution indicating that the speeds of sequential phases of motion are independent and biochemically well regulated. As a result we propose a model for motor driven lipid droplets that exhibits a sequential run behavior with occasional pauses.

DOI: 10.1103/PhysRevE.86.031910 PACS number(s): 87.64.−t, 87.15.hj, 87.16.Wd

I. INTRODUCTION

The finely controlled trafficking of cargoes within cells is crucial for a wide range of biological processes such as signaling, viral infection, and metabolism [1,2]. The motile processes involved are complex. Recent advances in instrumentation provide bright field optical microscopy with highly sensitive ultrafast complementary metal-oxide-semiconductor (CMOS) cameras and well collimated high luminosity light sources (wave guide coupled LED arrays) which when combined with sophisticated tracking software, provide nanometre resolution of organelle positions at sub-millisecond time scales in live cells. The development of robust automated particle tracking algorithms that are optimized for intracellular imaging then allows a vast amount of detailed information on the statistics of organelle motion inside these live cells to be collected [3]. For example, thousands of organelles can be tracked simultaneously in a single cell over several minutes, and information on the ensemble dynamics can be extracted [4].

The mean square displacement (MSD) is a commonly used statistical tool for determining the dynamic properties of stochastically fluctuating nanomotors [5,6]. Arcizet *et al.* [7] recently demonstrated a method whereby the motion of individual intracellular vesicles was analyzed by automatic segmentation into different regimes of motion and the MSDs were calculated in a time-resolved manner. It enabled retrieval of the speed distribution of the motor driven run-rest motion of vesicles over a reasonable range of time scales. However, the mean square displacement is known to be a relatively insensitive average measure of the length scale dependence of motile processes [4,8], and robust segmentation is challenging.

Another measure is the first-passage-probability $F(t,L)$, or FPP, defined as the probability per unit time (t) that a particle exceeds a displacement L from its origin for the first time [9]. Although this concept has long been applied to the modeling of motor protein dynamics [10,11], only recently has it been used for the analysis of ensembles of experimental particle tracking data on cargo trafficking within cells [4,8]. In contrast to the MSD, the FPP distribution can provide a detailed account of intracellular transit speeds, diffusivities, time and length scales. Furthermore the FPP can be used as an unbiased measure (without segmentation or the imposition of arbitrary parameters), unlike an equivalent MSD analysis. Although analysis of specific types of motility can be performed using MSD analysis, this requires presorting of data, which can introduce bias [7].

Subdiffusive motion is predominantly found for vesicle motion at short time scales within live cells whether the vesicles are actively or passively transported [3,6,12,13], and practically the motion is defined according to the exponent of power law fits to the MSD as a function of time ($\langle r^2\rangle \sim t^{\beta}$, where $\beta < 1$). Two separate theoretical scenarios [14–16] explain passive (thermal) subdiffusive behavior inside cells that cannot be differentiated on the basis of their MSDs alone: *continuous time random walks* with a power law wait time distribution (observed *in vitro* for the caged motion of colloids in actin gels [17,18]) and *Brownian walks on a fractal* ("an ant in a labyrinth") [19]. Clear theoretical predictions have been made for the mean first-passage time for the two separate subdiffusive processes [15]. A third possible theoretical scenario is related to the fractional Brownian motion or fractional Langevin equation, although we are not aware that any exact predictions have yet been made for the FPP distributions for such a system [20].

*t.a.waigh@manchester.ac.uk
†viki.allan@manchester.ac.uk

In this paper we calculate detailed high resolution FPP distributions, together with the MSDs and mean first-passage times (MFPTs), for the motion of single organelles inside live cells. We use this analysis to determine the varieties of stochastic motion observed in the congested environment of live cells at different time and length scales, and explore further the subdiffusive motion at short time scales by making use of the high data acquisition rates.

II. MATERIALS AND METHODS

An Olympus IX71 microscope was used with a fast Photron PCI 1024 CMOS camera (1–10^5 fps) and a bright LED array (525 nm, CoolLED PE-100). The microscope was mounted on an active vibration controlled optical table to remove external vibrations. Dynein-driven movement of lipid droplets was investigated in MRC-5 (human infantile lung) cells, grown on glass bottomed dishes (MatTek, Ashland, MA) in Hams F12 medium with 10% foetal bovine serum and incubated on the microscope at 37 °C. The movement was imaged at 10 000 frames per second by bright-field microscopy with a ×100 PLAN FLN objective lens (NA = 1.3), and a water immersion condenser (NA = 0.9), giving a resolution of 5.988 pixels per μm (charge-coupled device 512×512 pixels). The lipid droplet motion was subsequently analyzed using PolyParticleTracker [21], a MATLAB (MathWorks, USA)-based particle detection and tracking software that calculates the particle position based on a two-dimensional fourth order polynomial fit to the intensity that is weighted by a Gaussian function centered on the particle. The method is relatively insensitive to background light levels and is thus ideal for tracking in the inhomogeneous optical environment of the cell [21]. The MATLAB software was adapted to function on a parallel eight core computer architecture to improve the processing time of large data sets (>70 000 frames in a single movie). The positions of the particles were measured with a resolution in the range 5–10 nm which depended on the size and optical contrast of a particular organelle. Particles were selected where the movement was predominantly directed towards the cell's nucleus, and hence can be assumed to be dynein driven [4], although other motor proteins are known to be present in the system (kinesin and myosin) and may contribute towards any movement. The tracked particles were lipid droplets (as determined by specific Nile red staining control experiments; data not shown), chosen as they display good refractive index contrast [22]. The size of the lipid droplets was approximately 0.6 μm in diameter and these large organelles were expected to interact strongly with the mesh of the cytoskeleton in the surrounding environment in addition to the sections upon which they were tethered or moving.

III. RESULTS AND DISCUSSION

We calculated the FPP from the raw coordinate data from a selected track [Fig. 1(a)]. A multiple peaked distribution of inverse speeds was observed as a function of passage length, which would appear to correspond to different phases of motion due to the active transport of motor proteins. To determine the exact origin of these multiple peaks, we used a conventional method of displaying tracked progression. Using the coordinates to plot a track of the lipid droplet [Fig. 1(b), inset], we took a smooth contour along the track by averaging the coordinates within a one-pixel radius of each point [8], and then determined the position of the lipid droplet along the contour. When the displacement of the droplet was plotted versus time, we observed that the motion did indeed undergo distinct epochs of motion [Fig. 1(b)]. Using these epochs as a guide, we manually segmented the track and then calculated the FPP for the six individual sections of particle movement [see Fig. 1(a) inset for the FPP of section A; additional sections are shown in the Supplemental Material [23]]. The FPP of the separate sections revealed individual Gaussian peaks that correspond to the peaks already seen in the FPP of the full length of the track. Therefore the FPP alone of the complete track can be seen as a useful method for analyzing individual organelle motility and revealing different phases of motion. Although a similar distribution could be obtained from the

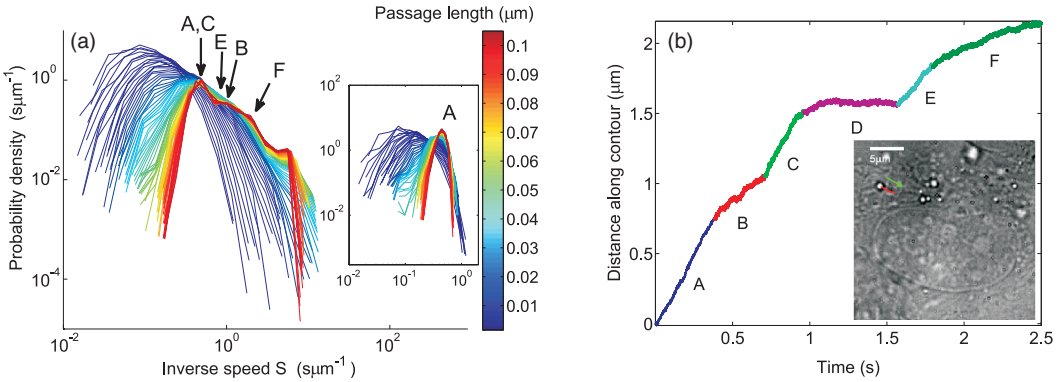

FIG. 1. (Color online) First-passage-probability of a lipid droplet in an MRC-5 cell (darker colors are short passage lengths and lighter colors are longer passages). (a) Multiple distinct peaks, labeled A–F, are detected in the FPP plot for the complete track. (b) The position in time of a lipid droplet along a smoothed contour (the microtubule). The inset shows the first frame of the cell image with the track superimposed (arrow indicates direction). The particle undergoes several distinct epochs of movement, labeled A–F, progressing different distances at different rates. The FPP of section A alone is shown in the inset in (a). See Supplemental Material, Appendix A [23], for additional examples. Each run section has a well defined Gaussian distribution. Section D does not generate a specific peak in (a), as it is a paused section of motion.

distance along a contour and segmenting the track, this requires arbitrary parameters which would affect the results and hence is less robust.

We have previously shown that the distribution of speeds for early endosomes in live cells, obtained using FPP, is heavily dependent on the distances traveled [4]. For the lipid droplet shown in Fig. 1, the largest variation in speed is observed at short length scales (around 0.01 μm), and these speeds conform to a log-normal distribution (in agreement with experiments for a passive diffusive process, shown in the Supplemental Material, Appendix B [23]). As the passage length increases, the distribution tends to narrow and multiple peaks appear in the speed distribution [Fig. 1(a)]. The radial fluctuations of the size of the lipid droplets determined by the tracking software are $<\sim$1.4% in Fig. 1, which provides a negligible change to the determination of the position of the optical center of the lipid droplet. The FPP, MFPT and MSDs are thus not noticeably affected by shape variations of the droplet (if they exist).

Further analysis of the FPP data for section A revealed that for short passages (of the order of 0.01 μm) a log-normal distribution of the inverse speeds was observed [Fig. 2(a)], in agreement with experiments for a passive diffusive process (see Supplemental Material, Appendix B [23]). For passages of the order of 0.1 μm and greater, we saw a single well defined Gaussian distribution for section A [Fig. 2(b)] and for all other sections except section D, where the particle was not undergoing directed movement. The multiple peaks of the speed distribution in the FPP over the full length of the motion [Fig. 1(a), A–F] are thus an independent summation of individual single Gaussians over each stretch. The speed in a single sequential run is well regulated ($+/-10\%$). The different peak positions for sequential runs may be due to the number of motor proteins attached at a given time, the type of motor protein attached, different stages of "gearing" of the individual motors, or the different viscoelastic environments encountered by the vesicle. Further examples of tracked lipid droplets exhibiting this behavior appear in the Supplemental Material, Appendix F [23].

As a control, we then compared the FPP distribution of motor-driven lipid droplets with that for purely diffusive motion (polystyrene beads in solution; see Supplemental Material, Appendix B). In this case the log-normal distribution for short time and short passage lengths observed for the actively transported lipid droplets persists over all passage lengths. We did not see a switch to a Gaussian distribution at longer length scales, unlike observations for the motor-driven organelle movement.

We are now in a position to explore in greater depth the nature of this motion. From calculations of the MSD and MFPTs over the full length of the track, we see evidence for subdiffusive passive (thermal) motion. For the MSD [Fig. 3(a)], at short time scales ($<$0.01 s) the exponent is less than 1, therefore subdiffusive, and at longer time scales ($>$0.01 s) the exponent is greater than 1, therefore active superdiffusive motion [12,13]. We believe that this is because at short time scales there are a multitude of fluctuating tethered motions of the lipid droplets attached to motor proteins that ultimately sum up to directed, driven movement at longer time scales. As only short displacements are achieved at such short time scales, those caused by motor driven movement are lost amongst these fluctuations. The time scale of the switch from passive subdiffusive motion to superdiffusive motion is set by the rate at which the motor proteins step and the amplitude of their stepping motion.

The MFPT distribution is shown in Fig. 3(b). When averaged over all six sections (A– F), at short times the data follows a power law $\langle t_{\mathrm{FPT}}\rangle \sim L^{\alpha}$. This is in agreement with a model for passive Brownian random walks on a fractal ($\langle t_{\mathrm{FPT}}\rangle \sim A + BL^{\alpha}$) and disagrees with the continuous time random walk model which predicts that the MFPT diverges [14,15]. It is also in agreement with simulations of a dynamic fluctuating protein fractal [16]. Furthermore, the full FPP is predicted to have an exponential long time tail with Brownian motion on a fractal, which is observed in the experimental data (see Supplemental Material, Appendix C). A power law tail, which is the prediction for continuous time random walks, is not a good fit to the data. We attribute the fractal nature of the Brownian motion to a combination of the congested environment inside the cell (e.g., the cytoskeleton) and the flexural modes of the microtubules to which the organelles are tethered [13]. At longer times the MFPT switches to

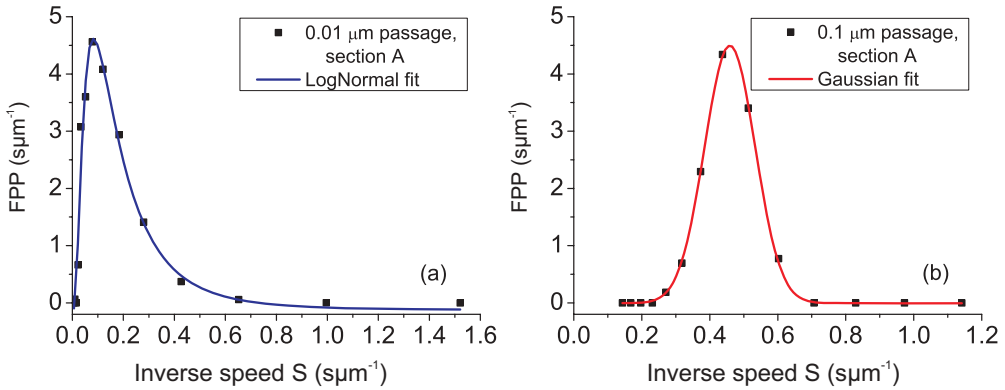

FIG. 2. (Color online) (a) First-passage-probability for a passage length of 0.01 μm for section A of the track. This distribution of inverse speeds can be described by a log normal distribution. (b) First-passage-probability for a passage length of 0.1 μm for section A of the track. This distribution of inverse velocities can be described by a Gaussian curve.

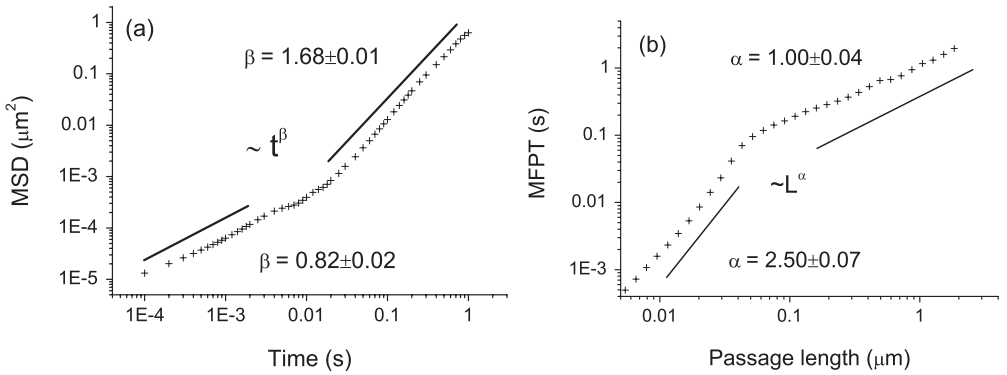

FIG. 3. (a) The mean square displacement of the complete track as a function of time. The motion is subdiffusive at short time scales (<0.01 s) and superdiffusive at longer time scales (>0.01 s). (b) The mean first-passage time of the track as a function of passage length. There is again a switch between two power law behaviors.

another power law behavior with an exponent approximately equal to 1 [Fig. 3(b)], corresponding to the active sub-ballistic superdiffusive, motor driven motion of the lipid droplets [24]. Recent theoretical work on continuous time random walks in confined geometries may improve the agreement with experiment for the passive subdiffusive motion, although to our knowledge no explicit FPP distributions of such behavior have yet been predicted [6].

An additional prediction is made in the literature for passive fractal Brownian walks that the exponents of the power law of the MFPT and MSD are $\alpha = 1/\nu$ and $\beta = 2\nu$, respectively [25–27], where ν is the walk dimension of the system. Walk exponents from the MSD and MFPT were therefore calculated at short times and compared (see Supplemental Material, Appendix D). Although the walk exponents from both methods were strongly correlated (Pearson correlation coefficient 0.94), they were not in perfect agreement. The average walk exponent was 0.12 for the MSD and 0.18 for the MFPT. Perfect agreement is predicted for the exponents by a general scaling calculation and exact renormalization group lattice calculations on specific fractal geometries (e.g., Sierpenski gasket) [19]. The disagreement is likely due to the approximate nature of the single fractal exponent used to describe the geometrical environment of a live cell over a range of length scales at short times, i.e., a multifractal approach is more appropriate [28].

Fractional Brownian motion provides another intriguing model for subdiffusive Brownian motion, since it provides a more natural description of the dynamics of polymeric tethers on the vesicle, e.g., a Rouse model for the motor protein tethers [29]. Initial results for the MFPT scaling in one dimension predict a similar dependence of the MFPT on the length (L) as for fractal Brownian motion [30]. An approximate result for the full FPP distribution predicts an exponential decay at long times again in agreement with our data [28]. However, more theoretical work is required to rigorously test the predictions of fractional Brownian motion for FPP distributions, although they are known to be closely related to continuous time random walks [31].

Another approach is to attribute all the particle motion to viscoelastic effects [32]. This often yields useful information, but practically data interpretation requires that the generalized Stokes-Einstein equation is invoked, which breaks down in a large variety of conditions and is fundamentally not valid on time scales where active driven motion is important. It will thus be avoided here.

Previously, a run-rest behavior was observed for Rab5 early endosomes in HeLaM and hTERT-RPE-1 cells [4,8], which had well defined rest periods. FPP analysis was applied to an ensemble of endosomes where characteristic speeds, diffusivities, time and length scales were observed. In contrast, here we have applied the same analysis to individual organelles, namely lipid droplets in MRC-5 cells, at much higher data acquisition rates (10 000 fps vs 28 fps). The lipid droplets display what we term sequential run behavior, where the droplets undertake consecutive periods of motion at distinct speeds, with only occasional pauses [Fig. 1(b)]. Switches in speed within individual endosome runs were also observed for some endosomes using manual analysis of tracks [4], meaning that such changes may be an inherent property of dynein-driven motility. The difference in motion between the two organelle types may be attributed to the larger size of the lipid droplets (600 versus 200 nm) which may have a greater number of motor proteins attached to the cargo in order to overcome a larger resistance to movement through the crowded cytoplasm. In support of this notion, the lipid droplets move more slowly (up to $\sim$2.0 μm s^{-1}) but more continuously than the endosomes, which have a peak speed of $\sim$8.0 μm s^{-1} [4] and yet stop and start more often.

IV. CONCLUSIONS

The FPP has the advantage over other methods of characterizing particle motion, such as the temporal MSD analysis used in [7], in that it does not require assumptions to be made about the particles' motion, nor does it use arbitrary parameters or thresholds. This could prove a useful tool for the study of intracellular particle dynamics, since it removes an ambiguity during the comparison of real data and predictive models. The high sampling speed of the camera in the current experiments allowed us to avoid ensemble averaging data over a highly diverse range of intracellular environments: i.e., the motion of single lipid vesicles could be analyzed. Additional useful

information is available from single particle tracking using complementary statistical analysis tools such as the mean maximum excursion method, kurtosis, and angular correlation functions [20,33–35]. These methods will be studied in detail in future work, but preliminary studies of the angular correlation functions of lipid droplets indicate good agreement with the current first-passage-probability study.

ACKNOWLEDGMENTS

We wish to thank Dr. S. Rogers for supplying the original MATLAB code for the first-passage-probability calculations and the PolyParticleTracker software [36]. We are also extremely grateful to Dr. N. Flores-Rodriguez and Dr. R. Neville for useful discussions and advice. This work was funded by the BBSRC.

[1] B. Alberts, A. Johnson, J. Lewis, M. Raff, K. Roberts, and P. Walter, *Molecular Biology of the Cell*, 4th ed. (Garland Science, New York, 2002).
[2] J. Howard, *Mechanics of Motor Proteins and the Cytoskeleton* (Sinauer Associates, Sunderland, MA, 2001).
[3] D. Wirtz, Annu. Rev. Biophys. **38**, 301 (2009).
[4] N. Flores-Rodriguez, S. S. Rogers, D. A. Kenwright, T. A. Waigh, P. G. Woodman, and V. J. Allan, PLoS ONE **6**, e24479 (2011).
[5] E. Sackmann, F. Keber, and D. Heinrich, in *Annu. Rev. Condens. Matter Phys.*, edited by J. Langer (Annual Reviews, Palo Alto, California, USA, 2010), Vol. 1, pp. 257–276.
[6] J.-H. Jeon, V. Tejedor, S. Burov, E. Barkai, C. Selhuber-Unkel, K. Berg-Sorensen, L. Oddershede, and R. Metzler, Phys. Rev. Lett. **106**, 048103 (2011).
[7] D. Arcizet, B. Meier, E. Sackmann, J. O. Rädler, and D. Heinrich, Phys. Rev. Lett. **101**, 248103 (2008).
[8] S. S. Rogers, N. Flores-Rodriguez, V. J. Allan, P. G. Woodman, and T. A. Waigh, Phys. Chem. Chem. Phys. **12**, 3753 (2010).
[9] S. Redner, *A Guide to First Passage Processes* (Cambridge University Press, Cambridge, UK, 2001).
[10] R. F. Fox and M. H. Choi, Phys. Rev. E **63**, 051901 (2001).
[11] A. G. Hendricks, B. I. Epureanu, and E. Meyhöfer, Nonlinear Dynam. **53**, 303 (2008).
[12] L. Bruno, V. Levi, M. Brunstein, and M. A. Despósito, Phys. Rev. E **80**, 011912 (2009).
[13] A. Caspi, R. Granek, and M. Elbaum, Phys. Rev. Lett. **85**, 5655 (2000).
[14] S. Condamin, O. Bénichou, V. Tejedor, R. Voituriez, and J. Klafter, Nature (London) **450**, 77 (2007).
[15] S. Condamin, V. Tejedor, R. Voituriez, O. Bénichou, and J. Klafter, Proc. Natl. Acad. Sci. USA **105**, 5675 (2008).
[16] S. Reuveni, R. Granek, and J. Klafter, Proc. Natl. Acad. Sci. USA **107**, 13696 (2010).
[17] E. R. Weeks and D. A. Weitz, Phys. Rev. Lett. **89**, 095704 (2002).
[18] I. Y. Wong, M. L. Gardel, D. R. Reichman, E. R. Weeks, M. T. Valentine, A. R. Bausch, and D. A. Weitz, Phys. Rev. Lett. **92**, 178101 (2004).
[19] D. ben-Avraham and S. Havlin, *Diffusion and Reactions in Fractals and Disordered Systems* (Cambridge University Press, Cambridge, UK, 2000).
[20] J.-H. Jeon and R. Metzler, Phys. Rev. E **81**, 021103 (2010).
[21] S. S. Rogers, T. A. Waigh, X. Zhao, and J. R. Lu, Phys. Biol. **4**, 220 (2007).
[22] M. A. Welte, Biochem. Soc. Trans. **37**, 991 (2009).
[23] See Supplemental Material at http://link.aps.org/supplemental/10.1103/PhysRevE.86.031910 for FPPs of individual epochs shown in Fig. 1, FPPs and MFPTs for diffusing latex spheres, and FPPs of additional tracks analyzed.
[24] R. Metzler and J. Klafter, J. Phys. A **37**, R161 (2004).
[25] B. Hughes, *Random Walks and Random Environments. Volume 1: Random Walks* (Oxford University Press, Oxford, United Kingdom, 1995).
[26] B. Hughes, *Random Walks and Random Environments. Volume 2: Random Environments* (Oxford University Press, Oxford, United Kingdom, 1996).
[27] J. Klafter and I. M. Sokolov, *First Steps in Random Walks* (Oxford University Press, Oxford, United Kingdom, 2011).
[28] S. C. Lim and S. V. Muniandy, Phys. Rev. E **66**, 021114 (2002).
[29] Y. Kantor and M. Kardar, Phys. Rev. E **76**, 061121 (2007).
[30] D. O'Malley, J. H. Cushman, and G. Johnson, J. Stat. Mech. (2011) L01001.
[31] R. Metzler and J. Klafter, Phys. Rep. **339**, 1 (2000).
[32] S. S. Rogers, T. A. Waigh, and J. R. Lu, Biophys. J. **94**, 3313 (2008).
[33] M. A. Despósito, C. Pallavicini, V. Levi, and L. Bruno, Physica A **390**, 1026 (2011).
[34] M. Magdziarz, A. Weron, K. Burnecki, and J. Klafter, Phys. Rev. Lett. **103**, 180602 (2009).
[35] V. Tejedor, O. Bénichou, R. Voituriez, R. Jungmann, F. Simmel, C. Selhuber-Unkel, L. B. Oddershede, and R. Metzler, Biophys. J. **98**, 1364 (2010).
[36] The MATLAB code for PolyParticleTracker and the first-passage-probability calculation may be found here: http://personalpages.manchester.ac.uk/staff/david.kenwright/.